Optimal aeration strategies of small-size wastewater treatment plants: influence of optimization time horizon

B. CHACHUAT, N. ROCHE and M.A. LATIFI*

Laboratoire des Sciences du Génie Chimique, CNRS-ENSIC, B.P. 451, 1 rue Grandville
54001 Nancy Cedex, France

Abstract

This paper presents the influence of time horizon on dynamic optimization of small-size wastewater treatment plants alternating aerobic and anoxic processes. The optimization problem consists in determining the aeration policy (air-on and air-off periods) that minimizes the energy dissipated by the aeration system subject to both effluent and operating constraints.. It was shown that although the optimized aeration policy obtained over short time horizons (*e.g.* 24 hours) leads to large reductions of energy consumption (up to 30%) with respect to the usual operating mode, its application over long time periods (*e.g.* 60 days) results in a washout of autotrophic bacteria, hence leading to a large exceeding of total nitrogen constraint. On the other hand, long time horizon optimized policies were shown to guarantee a durable functioning of the treatment plant. The resulting energy consumption savings are however lower (up to 15%), but are still important.

Key Words− Wastewater treatment ; Alternating activated sludge process ; Nutrient removal ; Energy consumption ; Dynamic optimization ; Short and long time horizons

---

*Author to whom all correspondence should be addressed, Tel: (+33) 03 83 17 52 34, Fax: (+33) 03 83 17 53 26, e-mail address : `latifi@ensic.inpl-nancy.fr`

1 Introduction

Since the new strict regulations on treated wastewater came out through the European Directive 91/271/EEC (which concerns mainly urban wastewater treatment), wastewater treatment industry, in Europe, has to face an important challenge arising from both regulation fulfillment and cost aspects of plant operation. These regulations hence give rise to both technical and economical problems since most of the exiting plants have to undertake major upgrading, particularly for nutrient removal. This is rather true for small-size wastewater treatment plants which are appropriate for communities of about $10,000$ p.e. (population-equivalent).

Most of municipal wastewater treatment plants use activated sludge process. More specifically, for small-size treatment facilities, the process generally consists of a single aeration basin configuration in which oxygen is either supplied by surface turbines or diffusers (Fig. 1). Nitrogen removal is realized by simply switching the aeration system *on* and *off* to create continuous alternating aerobic and anoxic conditions respectively. During switched-on periods, ammonium is converted into nitrate which is subsequently used to remove organic carbon in switched-off periods. An important feature of the alternating aerobic-anoxic process is its flexible control ability [1] which makes it suitable for optimization of operating costs.

[Figure 1 about here.]

Since the process consists of alternating aerated and non-aerated periods and since the aeration induces 60% to 80% of the global energy consumption (and subsequently operating costs) of a treatment plant [2], oxygen control is therefore of great importance. Most often, aeration sequencing is either performed by applying pre-specified on/off aeration periods or by defining switching values of redox potential or dissolved oxygen concentration, *etc.* [*e.g.,* 3; 4]. By means of the aforementioned controls, nitrogen concentration in the treated effluent may significantly exceed the allowed levels and the energy consumption may be very large.

An interesting alternative is to determine the aeration sequences which minimize the energy consumption and respect the effluent constraints. Such problem is referred to as a dynamic optimization problem or an open-loop optimal control problem. It consists in determining input profiles and/or parameters for a dynamic system (described by a detailed, typically nonlinear, differential equation model) that optimize its operation over some period of time according to a specified performance index [5]. Optimal control theory was introduced almost 40 years ago [6] and has been the subject of a large number of research contributions in the field of engineering. Recent examples in chemical engineering include design and operation of heat exchangers [7], determination of optimal grade transitions for a polymerization reactor [8], optimal control of batch electrochemical reactors [9], process safety analysis [10] and determination of optimal changeover policies [11].

In the field of wastewater treatment however, very few studies have been devoted to dynamic optimization despite the challenging problems posed by the design, optimization and control of wastewater treatment plants. This is rather true for small-size alternating aerobic-anoxic wastewater treatment plant [12].

In the present work, dynamic optimization of this class of treatment plants over long time horizons is addressed. This study is motivated by the fact that in a recent paper where we analyzed the feasibility of dynamic optimization of small-size wastewater treatment plants alternating aerobic and anoxic processes [13], we showed that the aeration rate (and hence energy consumption) may be reduced by up to 30% when optimized operating policies are applied with respect to usual operating modes. This result is true over a short time horizon, *i.e.* 24 hours, but there are no guarantees that the same results will be obtained over long time periods. Moreover, the crucial problem is to know if the functioning of the treatment plant is ensured when short time horizon optimized policies are recursively applied over long time periods, and how much would be the resulting benefits that may be realized upon the use of optimal strategies obtained over long time horizons.

The objective of this paper is to answer these questions by determining and comparing both short and long time horizons optimal aeration policies that minimize the energy consumption.

2 Process model

In this study, a real small-size treatment facility is considered (15, 000 p.e.). The process consists of a unique aeration tank ($V^{rb} = 2,050\,\mathrm{m}^3$) equipped with mechanical surface aerators (turbines) which provide oxygen ($\mathcal{P} = 30\,\mathrm{kW}$, $k_L a = 4.5\,\mathrm{h}^{-1}$) and mix the incoming wastewater with biomass (Fig. 1). The settler is a cylindrical tank where the solids are either recirculated to the aeration tank ($Q^{rs} = 7,600\,\mathrm{m}^3/\mathrm{day}$) or extracted from the system ($Q^w = 75\,\mathrm{m}^3/\mathrm{day}$).

The influent average flow $\left(\overline{Q^{in}}\right)$ is about $3,050\,\mathrm{m}^3/\mathrm{day}$ and average organic $\left(\overline{COD^{in}}\right)$ and nitrogen $\left(\overline{TN^{in}}\right)$ loads are $343\,\mathrm{mg/L}$ and $33\,\mathrm{mg/L}$ respectively (after primary treatment). The daily variations of dry weather conditions are based on measured data from the plant. It is accounted for by defining weighting functions for both influent flowrate and organic load variations, $\tau_Q(t)$ and $\tau_{COD}(t)$, (Fig. 2):

- *influent flowrate variation*:

$$Q^{in}(t) = \tau_Q(t)\,\overline{Q^{in}}\ ,\ \forall t \tag{1a}$$

$$\text{where} \quad \tau_Q(t) = \sum_{k=1}^{3}\left[a_k\,\cos(2k\pi t) + b_k\,\sin(2k\pi t)\right]$$

$$\text{with} \quad \begin{cases} a_1 = -0.32 & ; \quad b_1 = -0.18 \\ a_2 = 0.23 & ; \quad b_2 = -0.01 \\ a_3 = -0.06 & ; \quad b_3 = -0.01 \end{cases}$$

- <u>*organic load variation*</u>:

$$COD^{in}(t) \quad = \quad \tau_{COD}(t)\,\overline{COD^{in}}\ ,\ \forall t \tag{1b}$$

$$\text{where} \quad \tau_{COD}(t) \quad = \quad \sum_{k=1}^{3}\left[c_k\,\cos(2k\pi t) + d_k\,\sin(2k\pi t)\right]$$

$$\text{with} \qquad \begin{cases} c_1 = 0.24 & ;\ d_1 = -0.20 \\ c_2 = -0.09 & ;\ d_2 = 0.07 \\ c_3 = 0.04 & ;\ d_3 = -0.02 \end{cases}$$

- <u>*total nitrogen load variation*</u>:

  Since the concentration of total nitrogen in the influent exhibits small variations, it is assumed constant. Thus:

$$TN^{in}(t) \quad = \quad \overline{TN^{in}}\ ,\ \forall t \tag{1c}$$

[Figure 2 about here.]

The average wastewater composition is shown in Table 1. The fractions f are related to the state variables presented in Table 2 and defined as the ratio between the corresponding concentration and COD^{in} or TN^{in}.

[Table 1 about here.]

[Table 2 about here.]

The application of dynamic optimization methods requires the knowledge of a sufficiently accurate mathematical model. In this study, the biological reactor is described as a continuous stirred tank reactor (CSTR) and the biological processes are described by the generally accepted activated sludge model No.1 (ASM 1) [14]. Two restrictions are however brought to the original ASM 1 model: (i) the state variable describing total alkalinity is not included, and (*ii*) inert particulate material from influent and from biomass decay are combined into a single variable (X_I) since they are of minor interest. The resulting biodegradation model consists of 11 state variables and 20 parameters, respectively described in Table 2 and Table 3. The kinetic and stoichiometric parameter values considered are those defined for the *simulation benchmark* [15]. They can be found, for instance, on the European COST action 624 website (`http://www.ensic.u-nancy.fr/COSTWWTP`). In addition, the limitations induced on the heterotrophic biomass growth process by low concentration of ammonia in the reactor are taken into account by adding the factor $\frac{S_{NH}}{K_{NH,H}+S_{NH}}$ in the corresponding kinetic rate equation (see Appendix A). This modification requires an additional stoichiometric parameter $K_{NH,H}$, its value is set to $0.05\,\mathrm{g.m^{-3}}$ as suggested in [16] (Table 3).

[Table 3 about here.]

The degradation rates from the ASM 1 model are incorporated into mass balance equations for each component, assuming perfect mixing in the reactor:

$$\frac{dx_i^{br}}{dt} = \frac{Q^{in}x_i^{in} + Q^{rs}x_i^{rs} - \left(Q^{in} + Q^{rs}\right)x_i^{br}}{V^{br}} + \mathcal{R}_i \quad , \quad i = 1, 2, \ldots, 11 \tag{2}$$

where $\boldsymbol{x}^{in}$, $\boldsymbol{x}^{br}$ and $\boldsymbol{x}^{rs}$ are 11-dimensional vectors related to the concentration in the influent, in the reactor and in the recycled sludge respectively ; their components are (S_I S_S X_I X_S $X_{B,H}$ $X_{B,A}$ S_{NO} S_{NH} S_{ND} X_{ND} S_O)^T. $\boldsymbol{\mathcal{R}}$ is an 11-dimensional vector formed by the degradation rates of each component (see Appendix A).

The mass balance equation related to the concentration of dissolved oxygen may contain an additional term $\mathcal{A}_O$ which describes the oxygen transfer from the turbines:

$$\mathcal{A}_O = k_L a \left(S_O^{sat} - S_O\right) \tag{3}$$

where $k_L a$ is the oxygen transfer coefficient and S_O^{sat} is the saturated dissolved oxygen concentration ($S_O^{sat} = 10\,\mathrm{mg/L}$). Hence, the process is described by two models depending on whether the aeration system is on or off. Such systems are known as *hybrid discrete/continuous dynamic systems* [17].

The separation of liquid and solid phases which takes place in the settler is assumed to be perfect: (*i*) the sum of the two outflows (outlet and recycled sludge flowrates) equals the settler influent flowrate and (*ii*) the effluent is exclusively constituted by soluble components, *i.e.*

- *Effluent concentration*:

$$S_i^{eff} = S_i^{br} \tag{4a}$$

$$X_i^{eff} = 0 \tag{4b}$$

- *Recycled sludge concentration*:

$$S_i^{rs} = S_i^{br} \tag{5a}$$

$$X_i^{rs} = \frac{Q^{in} + Q^{rs}}{Q^{rs} + Q^{w}} X_i^{br} \tag{5b}$$

With these assumptions, the activated sludge process is described by two systems of ODE defined as:

$$\dot{\boldsymbol{x}} = \boldsymbol{f}^{(1)}(\boldsymbol{x}) \qquad \text{(air-on periods)} \tag{6a}$$

$$\dot{\boldsymbol{x}} = \boldsymbol{f}^{(2)}(\boldsymbol{x}) \qquad \text{(air-off periods)} \tag{6b}$$

where $\boldsymbol{f}^{(1)}$ and $\boldsymbol{f}^{(2)}$ are C^{∞} vector fields defined from $(\mathbb{R}^{+})^{11}$ to $\mathbb{R}^{11}$; their expressions are given in Appendix A.

3 Optimization problem statement

Organic and nitrogen removal is achieved by switching the turbines on and off, resulting in alternated aerobic-anoxic conditions in the aeration basin. Hence, the process can be seen as a succession of cycles where each cycle consists of an aeration period followed by a non-aeration period, *i.e.* the period between two consecutive starts of the turbines. Each cycle is then completely determined by means of two parameters. Thus, for a specified number N_c of cycles, the total number of parameters involved in optimization is $2 \times N_c$. In this work, the set of parameters which is considered is (Fig. 3):

- the duration ℓ^k of cycle k,
- the length of the aeration period a^k within the corresponding cycle.

[Figure 3 about here.]

The switching times t_b^k and t_c^k related to the end of the k-th aeration period and the end of k-th cycle are defined as:

$$t_b^k = t_0 + \sum_{j=1}^{k-1} \ell^j + a^k \tag{7a}$$

$$t_c^k = t_0 + \sum_{j=1}^{k} \ell^j \tag{7b}$$

Performance index

The objective of this study is to determine the aeration strategy that minimizes the operating costs of the process. The energy induced by the aeration process represents a significant part $(60 - 80\%)$ of the operating costs of the wastewater treatment plant. Therefore, the optimization of the aeration process can result in significant costs savings. Other costs such as those associated with pumping are neglected.

The energy $\mathcal{E}$ which is dissipated by the aeration system is defined as:

$$\mathcal{E} = \int_{t_0}^{t_f} \mathcal{P}(t) \, \mathrm{d}t \tag{8}$$

where $\mathcal{P}$ denotes the power consumption. Here, oxygen is provided in the reactor by surface turbines with fixed rotating speed. For typical values of the sludge concentration in the reactor (*e.g.* between 1 g/L and 5 g/L), the flow is shown to be turbulent and the power consumption is therefore independent on the sludge concentration:

$$\mathcal{P} = N_p \, \rho \, \mathcal{N}^3 \, d^5 \tag{9}$$

where N_p is the power number ($N_p = \mathrm{C}^{\underline{\mathrm{te}}}$), ρ the liquid density, $\mathcal{N}$ the aerator rotation speed and d the aerator diameter.

It is noteworthy that extra-power consumption induced by the starting process of the turbines is not accounted for in this work. Therefore, the energy consumption is directly proportional to the aeration time and for a given number N_c of cycles, one can express the energy consumption as:

$$\mathcal{E} = \mathcal{P} \sum_{k=1}^{N_c} a^k \tag{10}$$

The performance index $\mathcal{J}$ is here defined as the total aeration period divided by the time horizon:

$$\mathcal{J} = \sum_{k=1}^{N_c} a^k \Bigg/ \sum_{k=1}^{N_c} \ell^k \tag{11}$$

$\mathcal{J}$ is a dimensionless variable and can be seen as the aeration rate over the optimization horizon: the smaller the aeration rate, the larger the reduction of energy consumption.

Constraints

Two different sets of constraints are considered in order (*i*) to satisfy the requirements imposed on the residual concentrations in the effluent, and (*ii*) to ensure the feasibility of the computed aeration profiles.

Effluent requirements:

Stricter regulations have been imposed during the last decade by the European Union on the effluent of wastewater treatment plants. Agglomeration effluents with a population-equivalent greater than $2,000$ should respect a minimum of secondary treatment (biological treatment with a secondary settler). The standards in terms of COD, BOD_5 and SS (suspended solids) are given by:

$$\mathrm{COD_{max}} = 125\,\mathrm{mg/L} \tag{12a}$$

$$\mathrm{BOD_{5max}} = 25\,\mathrm{mg/L} \tag{12b}$$

$$\mathrm{SS_{max}} = 35\,\mathrm{mg/L} \tag{12c}$$

The limit values for nitrogen are 15 mg/L (measured as N) for agglomerations of p.e. between $10,000$ and $100,000$. However, it is worth noticing that an objective of 10 mg/L is often aimed at making the plant operation more flexible:

$$\mathrm{TN_{max}} = 10\,\mathrm{mg/L} \tag{12d}$$

Operating constraints:

Operating constraints are imposed along with the aforementioned constraints on maximum residual concentrations. The objective of these additional constraints is (*i*) to prevent the turbines from damaging and (*ii*) to include aspects which are not described by the model.

Two operating constraints deal with minimum air-on ($t^{\text{on}}_{\text{min}}$) and air-off ($t^{\text{off}}_{\text{min}}$) cycle time. These lower limits are defined to avoid too frequent cycling of the turbines. Moreover, the minimum air-on time must be long enough to re-aerate most of the activated sludge after anoxic periods and to ensure that biomass and substrate are conveniently mixed in the aeration tank. In this work, both air-on and air-off times are set to 15 minutes.

A maximum air-on time ($t^{\text{on}}_{\text{max}}$) is also defined to prevent the propellers from early wear or from damaging. The upper limit is set to 120 minutes. At last, it is worth noticing that too long non-stirring and non-aeration periods can induce floc sedimentation in the aeration tank as well as anaerobic conditions, hence modifying the degradation performances. In addition, the CSTR assumption may be no longer valid for too long non-stirring periods. Therefore, a maximum air-off ($t^{\text{off}}_{\text{max}}$) time of 120 minutes is considered.

Optimization method

Rigorously speaking, the computation of aeration and non-aeration sequences which minimize the energy consumption can be stated as a *mixed-integer dynamic optimization* (MIDO) problem since the optimal number of cycles N_c must be determined as well as the parameters a^k and ℓ^k. However, (non-convex) MIDO problems are known to be difficult to solve [18] and are currently under investigation. In this work, it has been chosen to keep the number of cycles constant in order to deal with a more regular optimization problem. The influence of the number of cycles on the result of the optimization is investigated by applying simple enumeration techniques. The computation of optimal aeration strategies for a varying number of cycles will be the topic for further research.

The dynamic optimization problem on a given time horizon $[t_0, t_f]$ can be stated as:

$$
\begin{array}{rrcl}
 & \min_{a^1,\ell^1,\ldots,a^{N_c},\ell^{N_c}} \mathcal{J} & = & \sum_{k=1}^{N_c} a^k \Big/ \sum_{k=1}^{N_c} \ell^k \\
\text{subject to :} & \dot{\boldsymbol{x}} & = & \boldsymbol{f}^{(1)}(\boldsymbol{x}) \quad \text{if } t \in \left[t_c^{k-1^+}, t_b^{k^-}\right] \ , \ k = \overline{1, N_c} \\
 & \dot{\boldsymbol{x}} & = & \boldsymbol{f}^{(2)}(\boldsymbol{x}) \quad \text{if } t \in \left[t_b^{k^+}, t_c^{k^-}\right] \ , \ k = \overline{1, N_c} \\
 & 0 & \leq & \mathrm{TN}_{\max} - \left[S_{NO}^{br}(t) + S_{NH}^{br}(t) + S_{ND}^{br}(t)\right] \ , \ \forall t \\
 & 0 & \leq & \mathrm{COD}_{\max} - \left[S_I^{br}(t) + S_S^{br}(t)\right] \ , \ \forall t \\
 & 0 & \leq & \mathrm{BOD}_{5\max} - 0.25\left[S_I^{br}(t) + S_S^{br}(t)\right] \ , \ \forall t \\
 & t_{\max}^{\mathrm{on}} & \geq & a^k \ \geq \ t_{\min}^{\mathrm{on}} \ , \ k = \overline{1, N_c} \\
 & t_{\max}^{\mathrm{off}} & \geq & \ell^k - a^k \ \geq \ t_{\min}^{\mathrm{off}} \ , \ k = \overline{1, N_c} \\
 & 0 & = & \sum_{k=1}^{N_c} \ell^k - (t_f - t_0)
\end{array}
\tag{13}
$$

It is noteworthy that (13) is a smooth hybrid dynamic optimization problem, since switching instants t_b^k and t_c^k ($k = \overline{1, N_c}$) are determined by explicit conditions (7a) and (7b). Also note that the limitation on the residual concentration of suspended solids is not included in the optimization problem, since dynamic models $\boldsymbol{f}^{(1)}$ and $\boldsymbol{f}^{(2)}$ do not deal with particulate material in the effluent (the settler is assumed to work perfectly). The three remaining effluent requirements on COD, BOD_5 and TN are inequality path constraints that can be written in a general form as:

$$
N(\boldsymbol{x}) - N_{\max} \ \leq \ 0 \tag{14}
$$

To solve the dynamic optimization problem, these constraints are converted into integral path constraints defined as :

$$
g \ = \ \int_{t_0}^{t_f} \mathcal{L}(\boldsymbol{x})\, \mathrm{d}t \ = \ \int_{t_0}^{t_f} \max\left[N(\boldsymbol{x}) - N_{\max}\, ;\, 0\right]^2 \mathrm{d}t \tag{15}
$$

The resulting parametric optimization problem is solved by a successive quadratic programming (SQP) method – in this work, the `NLPQL` method [19] is used –. The gradients of the performance index and constraints with respect to the parameters are therefore required. Since the performance index and the operating constraints are independent on the state of the system, their gradients are obtained by simple differentiation. On the other hand, the gradients of the integral constraints (15) are computed by applying the adjoint system approach [*e.g.,* 5; 20] which is well suited for large-scale optimization problems:

$$\nabla_{a^k} g = \left[\mathcal{H}^{(1)}\big|_{t_b^{k-}} - \mathcal{H}^{(2)}\big|_{t_b^{k+}} \right] \tag{16a}$$

$$\nabla_{\ell^k} g = \sum_{j=k+1}^{N_c} \left[\mathcal{H}^{(1)}\big|_{t_b^{j-}} - \mathcal{H}^{(2)}\big|_{t_b^{j+}} \right] - \sum_{j=k}^{N_c} \left[\mathcal{H}^{(1)}\big|_{t_c^{j+}} - \mathcal{H}^{(2)}\big|_{t_c^{j-}} \right] - \mathcal{L}\big|_{t_c^{N_c}} \tag{16b}$$

where the Hamiltonians $\mathcal{H}^{(1)}$ and $\mathcal{H}^{(2)}$ are defined as:

$$\mathcal{H}^{(1)}(\boldsymbol{x}, \boldsymbol{\lambda}) = \mathcal{L}(\boldsymbol{x}) + \boldsymbol{\lambda}^T \boldsymbol{f}^{(1)}(\boldsymbol{x}) \tag{16c}$$

$$\mathcal{H}^{(2)}(\boldsymbol{x}, \boldsymbol{\lambda}) = \mathcal{L}(\boldsymbol{x}) + \boldsymbol{\lambda}^T \boldsymbol{f}^{(2)}(\boldsymbol{x}) \tag{16d}$$

and where $\boldsymbol{\lambda}$ is an 11-dimensional vector of costate variables defined as:

$$\dot{\boldsymbol{\lambda}}^T = -\frac{\partial \mathcal{H}^{(1)}}{\partial \boldsymbol{x}^T} \quad \text{if } t \in \left[t_c^{k-1^+}, t_b^{k-} \right], \; k = \overline{1, N_c} \tag{16e}$$

$$\dot{\boldsymbol{\lambda}}^T = -\frac{\partial \mathcal{H}^{(2)}}{\partial \boldsymbol{x}^T} \quad \text{if } t \in \left[t_b^{k+}, t_c^{k-} \right], \; k = \overline{1, N_c} \tag{16f}$$

with the following boundary conditions:

$$\boldsymbol{\lambda}(t_f) = \boldsymbol{0} \tag{16g}$$

$$\boldsymbol{\lambda}\left(t_b^{k+}\right) = \boldsymbol{\lambda}\left(t_b^{k-}\right) \quad k = \overline{1, N_c} \tag{16h}$$

$$\boldsymbol{\lambda}\left(t_c^{k+}\right) = \boldsymbol{\lambda}\left(t_c^{k-}\right) \quad k = \overline{1, N_c - 1} \tag{16i}$$

The integration of both state (6a)-(6b) and adjoint systems (16e)-(16f) is performed using `DASSL` solver [21] since these dynamic systems can be stiff in the neighborhood of switching times t_b^k and t_c^k, *e.g.* for the concentration of dissolved oxygen and its associated costate variable. Further details on the computation of the gradients can be found in [13].

It has to be clear that global optimality of the computed aeration profiles is in no way guaranteed, due to the application of a local gradient search method. The problem may exhibit several local minima, induced by the non-linearity of the dynamic model.

4 Optimization results

4.1 Optimal aeration strategies over short time horizons

Initial conditions considered in this work are given in Table 4. Note that the same set of initial conditions is always used in this work so that the results obtained can be compared.

[Table 4 about here.]

Optimal aeration profiles have been computed for different values of N_c by applying simple enumeration techniques. The corresponding values of the performance index for a 24-hour optimization are given in Fig. 4. The global aeration rate (performance index) first decreases as the number of cycles increases (from 12 to 29 cycles a day), since additional cycles increase the flexibility of the aeration policy. From 29 cycles, lower bounds $t_{\min}^{\text{on}}$ on parameters a^k are reached and extra-cycles then induce higher aeration rates. The optimal number of cycles over 24 hours is found to be 29 cycles and the corresponding aeration rate is $\mathcal{J} = 31.08\%$. However, it is worth noticing that N_c has an insignificant effect (between 12 and 30 cycles a day) on the optimal value of the performance index.

[Figure 4 about here.]

The influence of the minimum air-on time has also been investigated. Optimal aeration profiles have been computed for $t_{\min}^{\text{on}} = 5$, 10, 15, 20 and 30 minutes. The resulting optimal number of cycles and performance indexes are given in Table 5. Again, it can be seen that $t_{\min}^{\text{on}}$ has a small influence on the result of the optimization, since optimal aeration rates vary from $\mathcal{J} = 30.3\%$ to 32.1%.

[Table 5 about here.]

Subsequent results are given for 29 cycles a day (optimal value of N_c for $t_{\min}^{\text{on}} = 15$ min.). The optimal aeration policy and the corresponding aeration rates for each cycle are displayed in Fig. 5. It can be seen that optimization leads to high aeration rates between 4 *a.m.* and 4 *p.m.* (around 50%) whereas low aeration levels (about 10%) are applied at the beginning and at the end of the optimization period.

[Figure 5 about here.]

The corresponding effluent concentrations of total nitrogen, COD and BOD_5 are shown in Fig. 6. Note that all effluent criteria are satisfied. However, effluent constraints on both COD and BOD_5 remain always inactive (so these constraints are removed from the optimization problem), whereas the maximum allowed concentration of total nitrogen (10 mg/L) is reached at the beginning and at the end of the optimization period.

[Figure 6 about here.]

It is interesting to compare both total nitrogen and autotrophic biomass concentration profiles (Fig. 6 and Fig. 7). Low aeration rates lead to a sharp decrease in the concentration of autotrophic biomass, while the concentration of total nitrogen approaches 10 mg/L. Conversely, the concentration of autotrophic biomass increases when high aeration rates are imposed and the maximum allowed concentration of total nitrogen is no longer constraining. One should also note that the concentration of autotrophic biomass in the system is globally decreasing during the optimization period. This important issue will be discussed later.

[Figure 7 about here.]

The convergence of the solution to the optimal aeration profile generally requires large amounts of CPU time. Thus, several hundreds of iterations are required to solve the NLP problem using SQP method, and each SQP iteration requires between 10 and 20 seconds of CPU time of a PIII-500MHz PC, mainly due to small time steps ($dt = 1s$) used to compute accurate gradient estimation . Therefore, the computation of a single aeration profile may take several hours! The optimization problem should then be simplified.

4.2 Simplification of the optimization problem

To reduce the computation load required to compute optimal aeration profiles, a simplification of the optimization problem has been investigated. Equal length cycles $\ell^0 = \frac{t_f - t_0}{N_c}$ are considered instead of varying length cycles $(\ell^1, \ldots, \ell^{N_c})$. The set of optimization parameters is therefore reduced from $2 \times N_c$ to N_c parameters. Moreover, since inactive effluent constraints on COD and BOD_5 are dropped, the simplified optimization problem can be stated as:

$$
\begin{aligned}
\min_{a^1,\ldots,a^{N_c}} \mathcal{J} &= \sum_{k=1}^{N_c} a^k \Big/ N_c\,\ell^0 \\
\text{subject to :} \quad \dot{\boldsymbol{x}} &= \boldsymbol{f}^{(1)}(\boldsymbol{x}) \quad \text{if } t \in \left[t_c^{k-1^+}, t_b^{k^-}\right] \ , \ k = \overline{1, N_c} \\
\dot{\boldsymbol{x}} &= \boldsymbol{f}^{(2)}(\boldsymbol{x}) \quad \text{if } t \in \left[t_b^{k^+}, t_c^{k^-}\right] \ , \ k = \overline{1, N_c} \\
0 &\leq \mathrm{TN}_{\max} - \left[S_{NO}^{br}(t) + S_{NH}^{br}(t) + S_{ND}^{br}(t)\right] \ , \ \forall t \\
t_{\max}^{\text{on}} &\geq a^k \geq t_{\min}^{\text{on}} \ , \ k = \overline{1, N_c} \\
t_{\max}^{\text{off}} &\geq \ell^0 - a^k \geq t_{\min}^{\text{off}} \ , \ k = \overline{1, N_c}
\end{aligned}
\tag{17}
$$

The computational solution of problem (17) is performed in a similar way as problem (13), by converting the inequality state constraints into integral path constraints (15) and applying an SQP-based method. Computational times are greatly reduced, since the computation of problem (17) takes only about 30 minutes of CPU time for a 24-hour optimization problem.

In this case, the minimal aeration rate obtained for 15 cycles over a 24-hour period is $\mathcal{J} = 31.72\%$. It is noteworthy that this optimum is close to the one of the original optimization problem (13) ($\mathcal{J} = 31.08\%$), hence justifying the assumption of equal length cycles. In addition, both aeration and total nitrogen concentration profiles are similar to those obtained for problem (13) (Fig. 5 and Fig. 6). Again, high aeration rates are applied between 4 *a.m.* and 4 *p.m.*, while low aeration rates are observed at the beginning and at the end of the optimization period.

Recursive implementation of the optimal aeration strategy has been applied over 30 days, in order to investigate long-term effects of the optimization on the treatment plant functioning. Both profiles of autotrophic biomass and total nitrogen concentrations are given in Fig. 8. It can be seen that the application of the optimal aeration policy eventually results in a washout of autotrophic bacteria and consequently, the concentration of total nitrogen rapidly exceeds the constraint. The computation of optimal aeration profile over a 24-hour period does not really take into account the slow biological processes such as growth and decay of autotrophic bacteria. The determination of optimal aeration strategies over long time periods is therefore required.

[Figure 8 about here.]

4.3 Optimal aeration strategies over long time horizons

Solving problems (13) or (17) over long time horizons, such as tens of days, would give rise to optimization problems with hundreds of parameters. An alternative method consists of computing the 24-hour aeration policy (N_c cycles) which satisfies effluent requirements and operating constraints over long time periods. Over N_d days, switching times t_b^k and

t_c^k are defined as:

$$t_b^{(j-1)N_c+k} = t_0 + [(j-1)\,N_c + (k-1)]\,\ell^0 + a^k \qquad k = \overline{1, N_c}\ ,\ j = \overline{1, N_d} \quad \text{(18a)}$$
$$t_c^{(j-1)N_c+k} = t_0 + [(j-1)\,N_c + (k-1)]\,\ell^0 \qquad k = \overline{1, N_c}\ ,\ j = \overline{1, N_d} \quad \text{(18b)}$$

and the optimization problem can be stated as:

$$\begin{aligned}
\min_{a^1,\ldots,a^{N_c}} \mathcal{J} &= \sum_{k=1}^{N_c} a^k \Big/ N_c\,\ell^0 \\
\text{subject to:} \quad \dot{\boldsymbol{x}} &= \boldsymbol{f}^{(1)}(\boldsymbol{x}) \quad \text{if } t \in \left[t_c^{k-1^+}, t_b^{k^-}\right]\ ,\ k = \overline{1, N_c \times N_d} \\
\dot{\boldsymbol{x}} &= \boldsymbol{f}^{(2)}(\boldsymbol{x}) \quad \text{if } t \in \left[t_b^{k^+}, t_c^{k^-}\right]\ ,\ k = \overline{1, N_c \times N_d} \\
0 &\leq \mathrm{TN}_{\max} - \left[S_{NO}^{br}(t) + S_{NH}^{br}(t) + S_{ND}^{br}(t)\right]\ ,\ \forall t \\
t_{\max}^{\text{on}} &\geq a^k \geq t_{\min}^{\text{on}}\ ,\ k = \overline{1, N_c} \\
t_{\max}^{\text{off}} &\geq \ell^0 - a^k \geq t_{\min}^{\text{off}}\ ,\ k = \overline{1, N_c}
\end{aligned} \tag{19}$$

The computation of optimal aeration policy over 60 days (for 15 cycles a day) yields a minimum aeration rate of about $\mathcal{J} = 39.76\%$. Note that, this value is appreciably larger than the one obtained over a 24-hour period ($\mathcal{J} = 31.72\%$), since the slow dynamics of the process are taken into account in this case. Also note that the resulting aeration profile (Fig. 9) is somewhat different from those computed over short time periods (see Fig. 5). In this case, the largest aeration rates are applied during the night, in order to anticipate midday peak flowrate.

[Figure 9 about here.]

Both autotrophic biomass and total nitrogen concentration profiles over 60 days are given in Fig. 10. It can be seen that the concentration of autotrophic biomass is brought to a steady state value of about 90 mg.L^{-1} which corresponds to an appropriate functioning of the activated sludge process. During this period, the decay of autotrophic bacteria induce an increase in the concentration of total nitrogen, which eventually reaches the limit at the end of the optimization period.

[Figure 10 about here.]

For the test scenario adopted in this work, the minimum aeration time which guarantees durable functioning of the treatment plant and satisfies effluent requirements is around $9h30$ a day.

4.4 Potential benefits

It is interesting to quantify the benefits that may be realized when the long time horizon optimized aeration policy is used instead of the usual rule-based operating mode of small-size wastewater treatment plants. The usual operating mode consists of (i) the use of fixed and equal cycle lengths, and (ii) the maintain of aeration periods until a specified condition is fulfilled within each cycle, *e.g.* maximal concentration of dissolved oxygen, minimum value of redox potential, *etc...* In this work, 12 cycles a day ($\ell^0 = 120$ min.) are considered and the specified condition is the maximal concentration of dissolved oxygen which is set to 2 mg/L.

It should be noticed that unlike the optimized aeration strategy, the usual operating mode is a feedback control strategy since a measurement, *i.e.* dissolved oxygen concentration, is carried out before taking any decision on the aeration status (*on* or *off*). Despite this important detail, the resulting aeration time from the usual operating mode is compared to the one derived from the optimized operating mode on Fig. 11. Thus, the system is brought to its steady state (stabilization of autotrophic and heterotrophic biomass concentrations) by the controlled process over a long time period. The application of the rule-based operating mode leads to a global aeration rate of about 46.65%, *i.e.* a daily aeration time around $11h10$. Moreover, the residual concentration of total nitrogen in the effluent exceeds 10 mg/L during more than 2 hours.

[Figure 11 about here.]

On the other hand, it was shown that the application of the optimized operating mode yields a daily aeration time of about $9h30$ with fulfilled effluent constraints. Moreover, the durability of the plant functioning is guaranteed and large reductions in aeration time, up to 15%, may therefore be realized with respect to the usual operating mode, thus enabling significant cost savings. It should however be noticed that the real benefits will probably be lower than those determined without taking into account the effect of unknown disturbances and plant model mismatch. The robust closed-loop optimal control is the issue of the work that is currently undertaken.

5 Conclusions and perspectives

In this paper the use of dynamic optimization methods to determine optimal aeration strategies for small-size activated sludge treatment plants is presented. The optimization problem consists in determining the lengths of air-on and air-off periods that minimize the energy dissipated in the aeration system and satisfy constraints on the residual concentrations in the effluent as well as operating constraints.

Optimization over short time horizons is first discussed. It is demonstrated that aeration rates of 31%, *i.e.* $7h30$ of aeration time per day, are enough to ensure constraints fulfillment over 24 hours. However, too short aeration periods lead to a sharp decrease in autotrophic biomass which eventually result in a wash-out of autotrophic bacteria. Therefore, the determination of optimal aeration profiles over long time periods is investigated. It is shown that aeration rates of about 39.8% are required to guarantee a durable functioning of the treatment plant.

As usual operating modes (*e.g.* dissolved oxygen control) provide aeration rates 15% higher and are likely to exceed effluent constraints, it was demonstrated that the use of model-based optimization can greatly improve both performances and reliability of small-size wastewater treatment plants.

Note that the resulting optimal aeration profiles can be directly used as set-point profiles in an open-loop control strategy. However, due to large flowrate and load variations as well as plant-model mismatch, the open-loop control strategy may be inadequate. The embedding of optimal strategy in an advanced (tracking and eventually adaptive) nonlinear controller is therefore required to guarantee good performances (robustness) of the control system. On-line implementation of optimal control strategies will be the topic for further research.

Acknowledgments– The authors are grateful to *Ministère de l'Enseignement Supérieur et de la Recherche* (MESR) for its financial support.

Nomenclature

Roman symbols

a^k	=	aeration length within cycle k (s)
$\mathcal{A}_O$	=	oxygen transfer rate from the turbines $\left(\text{mg.L}^{-1}\text{.day}^{-1}\right)$
BOD_5	=	biochemical oxygen demand $\left(\text{mg.L}^{-1}\right)$
COD	=	chemical oxygen demand $\left(\text{mg.L}^{-1}\right)$
$\mathcal{E}$	=	energy consumption (J)
$\mathcal{J}$	=	performance index (−)
k_La	=	oxygen transfer coefficient $\left(\text{h}^{-1}\right)$
ℓ^k	=	total length of cycle k (s)
N_c	=	number of cycles (−)
N_d	=	number of days (−)
$\mathcal{P}$	=	nominal power of the turbines (kWh)
p.e.	=	population-equivalent

Q = flowrate $\left(\text{m}^3.\text{day}^{-1}\right)$

S_I = soluble inert COD concentration $\left(\text{mg.L}^{-1}\right)$

S_{ND} = soluble organic nitrogen concentration $\left(\text{mg.L}^{-1}\right)$

S_{NH} = ammonium concentration $\left(\text{mg.L}^{-1}\right)$

S_{NO} = nitrate and nitrite nitrogen concentration $\left(\text{mg.L}^{-1}\right)$

S_O = dissolved oxygen concentration $\left(\text{mg.L}^{-1}\right)$

S_O^{sat} = saturated dissolved oxygen concentration $\left(\text{mg.L}^{-1}\right)$

S_S = readily biodegradable COD concentration $\left(\text{mg.L}^{-1}\right)$

SS = suspended solids $\left(\text{mg.L}^{-1}\right)$

TN = total nitrogen $\left(\text{mg.L}^{-1}\right)$

t_b^k = turbines' switching-on time within cycle k (s)

t_c^k = turbines' switching-off time within cycle k (s)

$t_{\text{min}}^{\text{off}}$ = minimum length of air-off periods (s)

$t_{\text{max}}^{\text{off}}$ = maximum length of air-off periods (s)

$t_{\text{min}}^{\text{on}}$ = minimum length of air-on periods (s)

$t_{\text{max}}^{\text{on}}$ = maximum length of air-on periods (s)

V^{rb} = bioreactor volume (m^3)

$X_{B,H}$ = heterotrophic biomass concentration $\left(\text{mg.L}^{-1}\right)$

$X_{B,A}$ = autotrophic biomass concentration $\left(\text{mg.L}^{-1}\right)$

X_I = particulate inert COD concentration $\left(\text{mg.L}^{-1}\right)$

X_{ND} = particulate organic nitrogen concentration $\left(\text{mg.L}^{-1}\right)$

X_S = slowly biodegradable COD concentration $\left(\text{mg.L}^{-1}\right)$

Greek letters

τ_{COD} = influent COD concentration variation $(-)$

τ_Q = influent flowrate variation $(-)$

Subscripts and superscripts

$^{(1)}$ = air-on periods

$^{(2)}$ = air-off periods

^{in} = influent

^{max} = maximum value

^{rs} = recycled sludge

^{w} = excess sludge

$\bar{}$ = mean value

References

[1] Hao O.J., Huang J., *Alternating aerobic-anoxic process for nitrogen removal : Process evaluation*, Water Environ. Res., 68(1), (1996), 83–93

[2] Vasel J.L., *Contribution à l'étude des transferts d'oxygène en gestion des eaux*, , Fondation Universitaire Luxemourgeoise, Luxembourg, Arlon (1988)

[3] Héduit A., Duchêne P., Sintes L., *Optimization of nitrogen removal in small activated sludge plants*, Wat. Sci. Tech., 22(3-4), (1990), 123–130

[4] Lefèvre F., Audic J.M., Bujon B., *Automatic regulation of activated sludge aeration - Single-tank nitrification-denitrification*, Wat. Sci. Tech., 28(10), (1993), 289–298

[5] Bryson A.E., Ho Y.C., *Applied Optimal Control. Optimization, Estimation and Control*, Hemisphere Publishing Corporation (1975)

[6] Pontryagin L.S., Boltyanskii V., Gamkrelidze R., Mishchenko E., *The Mathematical Theory of Optimal Processes*, Pergamon Press, New York (1964)

[7] Georgiadis M.C., Rotstein G.E., Macchietto S., *Optimal design and operation of heat exchangers under milk fouling*, AIChE Journal, 44(9), (1998), 2099–2111

[8] Takeda M., Ray H., *Optimal-grade transition strategies for multistage polyolefin reactors*, AIChE Journal, 45(8), (1999), 1776–1793

[9] Fournier F., Latifi M.A., Valentin G., *Methodology of dynamic optimisation and optimal control of batch electrochemical reactors*, Chem. Engng. Sci., 54, (1999), 2707–2714

[10] Abel O., Marquardt W., *Scenario-integrated modeling and optimization of dynamic systems*, AIChE Journal, 46(4), (2000), 803–823

[11] Fikar M., Latifi M.A., Corriou J.P., *CVP-based optimal control of an industrial depropanizer column*, Comp. & Chem. Engng., 24, (2000), 909–915

[12] Kim H., McAvoy T., Anderson J., Hao O., *Control of an alternating aerobic-anoxic activated sludge system – part 2: optimization using a linearized model*, Control Engineering Practice, 8, (2000), 279–289

[13] Chachuat B., Roche N., Latifi M.A., *Dynamic optimisation of small size wastewater treatment plants including nitrification and denitrification*, Comp. & Chem. Engng., 25, (2001), 585–593

[14] Henze M., Grady C.P.L., Gujer W., Marais G.v.R., Matsuo T., *Activated Sludge Model No. 1*, 1, IAWQ, London (1987)

[15] Alex J., Béteau J.F., Copp J., Hellinga C., Jeppsson U., Marsili-Libelli S., Pons M.N., Spanjers H., Vanhooren H., *Benchmark for evaluating control strategies in wastewater treatment plants*, *Proc. ECC'99*, Karlsruhe, Germany (1999)

[16] Julien S., *Modélisation et Estimation pour le Contrôle d'un Processus Boues Activées Eliminant l'Azote des Eaux Résiduaires Urbaines*, , Institut National Polytechnique de Toulouse, France (1997)

[17] Barton P.I., Pantelides C.C., *Modeling of discrete/continuous processes*, AIChE Journal, 40(6), (1994), 966–979

[18] Allgor R.J., Barton P.I., *Mixed-integer dynamic optimization. I: Problem formulation*, Comp. & Chem. Engng., 23, (1999), 567–584

[19] Schittkowski K., *NLPQL : a fortran subroutine solving constrained nonlinear programming problems*, Annals of Operations Research, 5(6), (1985), 485–500

[20] Ruban A.I., *Sensitivity coefficients for discontinuous dynamic systems*, Journal of Computers and Systems Sciences International, 36(4), (1997), 536–542

[21] Brenan K., Campbell S., Petzold L., *Numerical solution of initial value problem in differential-algebraic equations*, North-Holland, New York (1989)

Appendix A – Activated sludge model equations

Kinetic rates ρ_j for degradation process $j = 1, \ldots, 8$ are defined as:

$$\boldsymbol{\rho} = \begin{pmatrix} \mu_H \frac{S_S^{br}}{K_S+S_S^{br}} \frac{S_{NH}^{br}}{K_{NH,H}+S_{NH}^{br}} \frac{S_O^{br}}{K_{O,H}+S_O^{br}} X_{B,H}^{br} \\ \mu_H \frac{S_S^{br}}{K_S+S_S^{br}} \frac{S_{NH}^{br}}{K_{NH,H}+S_{NH}^{br}} \frac{K_{O,H}}{K_{O,H}+S_O^{br}} \frac{S_{NO}^{br}}{K_{NO}+S_{NO}^{br}} \eta_{NOg} X_{B,H}^{br} \\ \mu_A \frac{S_{NH}^{br}}{K_{NH,A}+S_{NH}^{br}} \frac{S_O^{br}}{K_{O,A}+S_O^{br}} X_{B,A}^{br} \\ b_H X_{B,H}^{br} \\ b_A X_{B,A}^{br} \\ \kappa_h S_{ND}^{br} X_{B,H}^{br} \\ K_a \frac{X_S^{br}/X_{B,H}^{br}}{K_X+X_S^{br}/X_{B,H}^{br}} \left(\frac{S_O^{br}}{K_{O,H}+S_O^{br}} + \eta_{NO,h} \frac{K_{O,H}}{K_{O,H}+S_O^{br}} \frac{S_{NO}^{br}}{K_{NO}+S_{NO}^{br}} \right) X_{B,H}^{br} \\ K_a \frac{X_{ND}^{br}/X_{B,H}^{br}}{K_X+X_S^{br}/X_{B,H}^{br}} \left(\frac{S_O^{br}}{K_{O,H}+S_O^{br}} + \eta_{NO,h} \frac{K_{O,H}}{K_{O,H}+S_O^{br}} \frac{S_{NO}^{br}}{K_{NO}+S_{NO}^{br}} \right) X_{B,H}^{br} \end{pmatrix}$$

The apparent reaction rates $\mathcal{R}_i$ for components $i = 1, \ldots, 11$ are then given by:

$$\boldsymbol{\mathcal{R}} = \begin{pmatrix} 0 \\ -\frac{1}{Y_H}(\rho_1 + \rho_2) + \rho_7 \\ fr_{XI}(\rho_4 + \rho_5) \\ (1 - fr_{XI})(\rho_4 + \rho_5) - \rho_7 \\ \rho_1 + \rho_2 - \rho_4 \\ \rho_3 - \rho_5 \\ -\frac{1-Y_H}{2.86\,Y_H}\rho_2 + \frac{1}{Y_A}\rho_3 \\ -i_{NBM}(\rho_1 + \rho_2) - \left(i_{NBM} + \frac{1}{Y_A}\right)\rho_3 + \rho_6 \\ -\rho_6 + \rho_8 \\ (i_{NBM} - fr_{XI}\, i_{NXI})(\rho_4 + \rho_5) - \rho_8 \\ -\frac{1-Y_H}{Y_H}\rho_1 - \frac{4.57-Y_A}{Y_A}\rho_3 \end{pmatrix}$$

By incorporating this rates in mass-balance equations for each component and assuming that the biological reactor is perfectly stirred, the model of the system can be stated as:

$$\begin{aligned} \dot{\boldsymbol{x}} &= \boldsymbol{f}^{(1)}(\boldsymbol{x}) \qquad \text{(aeration periods)} \\ \dot{\boldsymbol{x}} &= \boldsymbol{f}^{(2)}(\boldsymbol{x}) \qquad \text{(non-aeration periods)} \end{aligned}$$

where $\boldsymbol{f}^{(1)}$ and $\boldsymbol{f}^{(2)}$ are C^∞ vector fields from $(\mathbb{R}^+)^{11}$ to $\mathbb{R}^{11}$ whose expressions are given by:

- For soluble components $(i = 1, 2, 7, 8, 9)$:

$$f_i^{(1)}(\boldsymbol{x}) = f_i^{(2)}(\boldsymbol{x}) = \frac{Q^{in}}{V^{br}}\left(x_i^{in} - x_i^{br}\right) + \mathcal{R}_i$$

- For particulate components $(i = 3, 4, 5, 6, 10)$:

$$f_i^{(1)}(\boldsymbol{x}) = f_i^{(2)}(\boldsymbol{x}) = \frac{1}{V^{br}}\left[Q^{in}\left(x_i^{in} - x_i^{br}\right) + Q^{rs}\frac{Q^{in} - Q^{w}}{Q^{rs} + Q^{w}}x_i^{br}\right] + \mathcal{R}_i$$

- For dissolved oxygen concentration ($i = 11$):

$$
\begin{aligned}
f_{11}^{(1)}(\boldsymbol{x}) &= \frac{Q^{in}}{V^{br}}\left(x_{11}^{in} - x_{11}^{br}\right) + \mathcal{R}_{11} + \mathcal{A}_{\mathcal{O}} \\
f_{11}^{(2)}(\boldsymbol{x}) &= \frac{Q^{in}}{V^{br}}\left(x_{11}^{in} - x_{11}^{br}\right) + \mathcal{R}_{11}
\end{aligned}
$$

List of Tables

Table 1: Average inlet composition

COD^{in} fractions	
f_{SI}	5%
f_{SS}	35%
f_{XI}	10%
f_{XS}	35%
f_{XBH}	15%
f_{XBA}	0%

TN^{in} fractions	
f_{SNH}	66%
f_{SNO}	0%
f_{SND}	2%
f_{XND}	32%

Table 2: Model state variables

1.	Inert soluble organic matter, S_I $\left[\mathrm{gCOD.m^{-3}}\right]$
2.	Readily biodegradable substrate, S_S $\left[\mathrm{gCOD.m^{-3}}\right]$
3.	Inert particulate organic matter and products, X_I $\left[\mathrm{gCOD.m^{-3}}\right]$
4.	Slowly biodegradable substrate, X_S $\left[\mathrm{gCOD.m^{-3}}\right]$
5.	Active heterotrophic biomass, $X_{B,H}$ $\left[\mathrm{gCOD.m^{-3}}\right]$
6.	Active autotrophic biomass, $X_{B,A}$ $\left[\mathrm{gCOD.m^{-3}}\right]$
7.	Nitrate and nitrite nitrogen, S_{NO} $\left[\mathrm{gN.m^{-3}}\right]$
8.	Ammonium nitrogen, S_{NH} $\left[\mathrm{gN.m^{-3}}\right]$
9.	Soluble biodegradable organic nitrogen, S_{ND} $\left[\mathrm{gN.m^{-3}}\right]$
10.	Particulate biodegradable organic nitrogen, X_{ND} $\left[\mathrm{gN.m^{-3}}\right]$
11.	Dissolved oxygen, S_O $[\mathrm{gO_2.m^{-3}}]$

Table 3: Model parameters

	Stoichiometric parameters	
Y_H	0.67	Yield for heterotrophic biomass $[-]$
Y_A	0.24	Yield for autotrophic biomass $[-]$
fr_{XI}	0.08	Fraction of biomass leading to particulate products $[-]$
i_{NBM}	0.08	Mass of biomass per mass of COD in biomass $\left[gN.gCOD^{-1}\right]$
i_{NXI}	0.06	Mass of biomass per mass of COD in products from biomass decay $\left[gN.gCOD^{-1}\right]$
	Kinetic parameters	
μ_H	4.0	Maximum specific growth rate for heterotrophic biomass $\left[day^{-1}\right]$
b_H	0.3	Decay rate coefficient for heterotrophic biomass $\left[day^{-1}\right]$
K_S	10.0	Half-saturation coefficient for heterotrophic biomass $\left[gCOD.m^{-3}\right]$
$K_{NH,H}$	0.05	Ammonia half-saturation coefficient for heterotrophic biomass $\left[gN.m^{-3}\right]$
$K_{O,H}$	0.2	Oxygen half-saturation coefficient for heterotrophic biomass $\left[gO_2.m^{-3}\right]$
K_{NO}	0.5	Nitrate half-saturation coefficient for denitrifying heterotrophic biomass $\left[gN.m^{-3}\right]$
μ_A	0.5	Maximum specific growth rate for autotrophic biomass $\left[day^{-1}\right]$
b_A	0.05	Decay rate coefficient for autotrophic biomass $\left[day^{-1}\right]$
$K_{NH,A}$	1.0	Ammonia half-saturation coefficient for autotrophic biomass $\left[gN.m^{-3}\right]$
$K_{O,A}$	0.4	Oxygen half-saturation coefficient for autotrophic biomass $\left[gO_2.m^{-3}\right]$
η_{NOg}	0.8	Correction factor for μ_H under anoxic conditions $[-]$
η_{NOh}	0.8	Correction factor for hydrolysis under anoxic conditions $[-]$
κ_h	3.0	Maximum specific hydrolysis rate $\left[day^{-1}\right]$
K_X	0.1	Half-saturation coefficient for hydrolysis of slowly biodegradable substrate $[-]$
κ_a	0.05	Ammonification rate $\left[m^3.gCOD^{-1}.day^{-1}\right]$

Table 4: Initial concentrations in the aeration tank

	S_I	S_S	X_I	X_S	$X_{B,H}$	$X_{B,A}$
Conc. (mg/L)	17.98	2.27	2120.15	79.55	2238.65	115.18

	S_{NO}	S_{NH}	S_{ND}	X_{ND}	S_O
Conc. (mg/L)	0.02	9.70	0.14	6.29	0.00

Table 5: Influence of the minimum aeration time $t^{\text{on}}_{\min}$

$t^{\text{on}}_{\min}$	5 min.	10 min.	15 min.	20 min.	30 min.
Optimal value of N_c	87 cycles	44 cycles	29 cycles	22 cycles	15 cycles
Performance index	30.307%	30.724%	31.076%	31.338%	32.089%

List of Figures

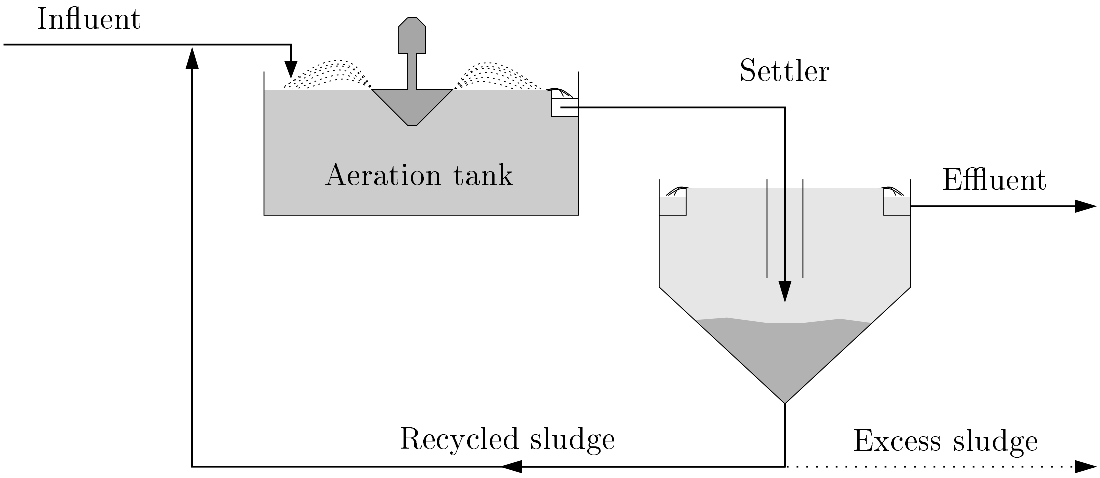

Figure 1: Typical small-size activated sludge treatment plant.

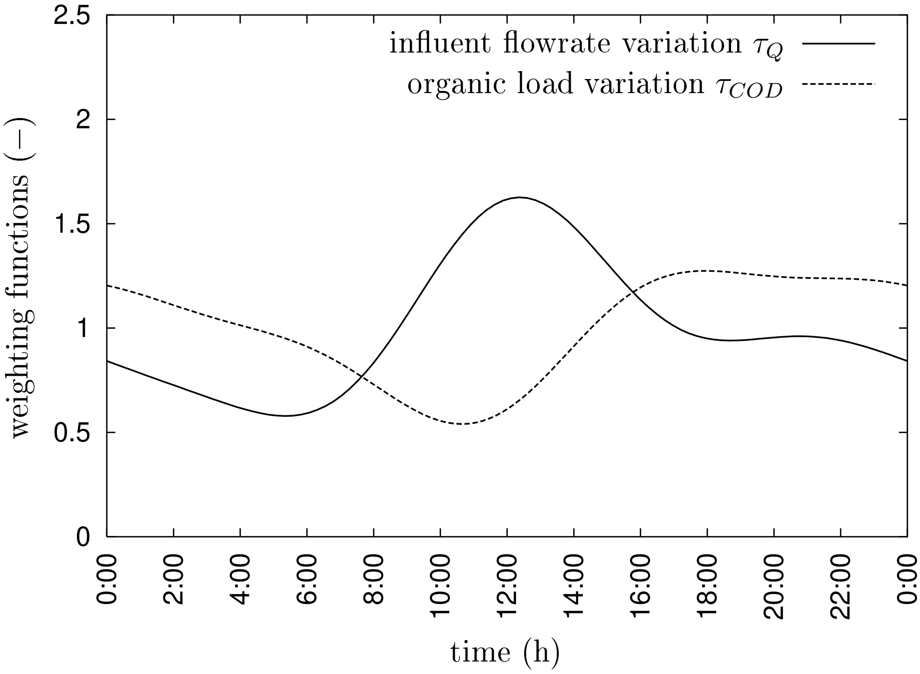

Figure 2: Influent flowrate and organic load variations.

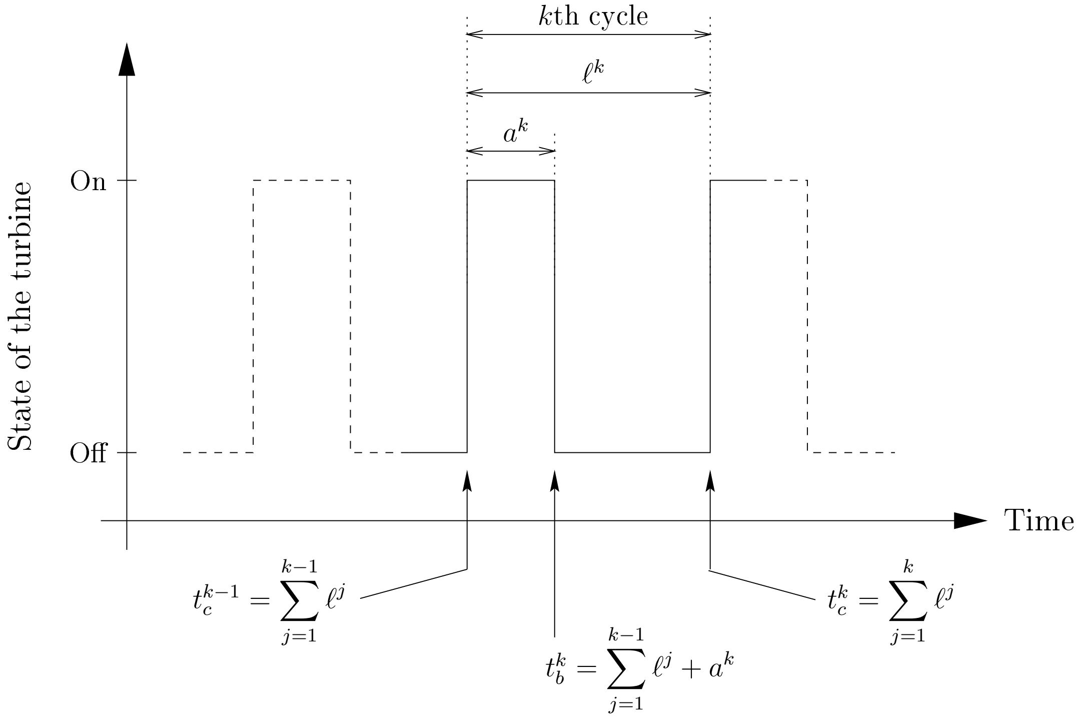

Figure 3: Optimization parameters.

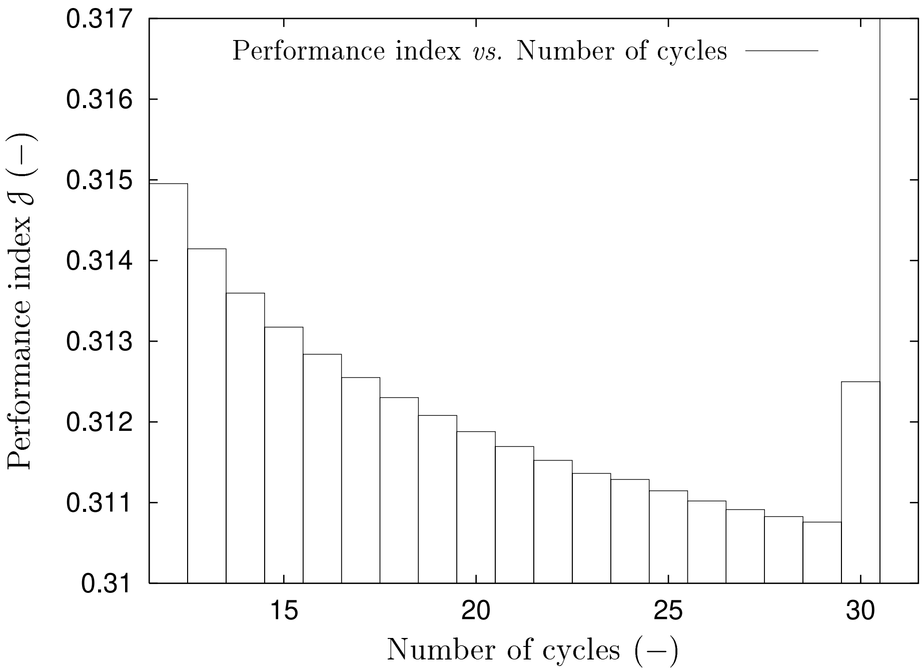

Figure 4: Performance index *vs.* Number of cycles.

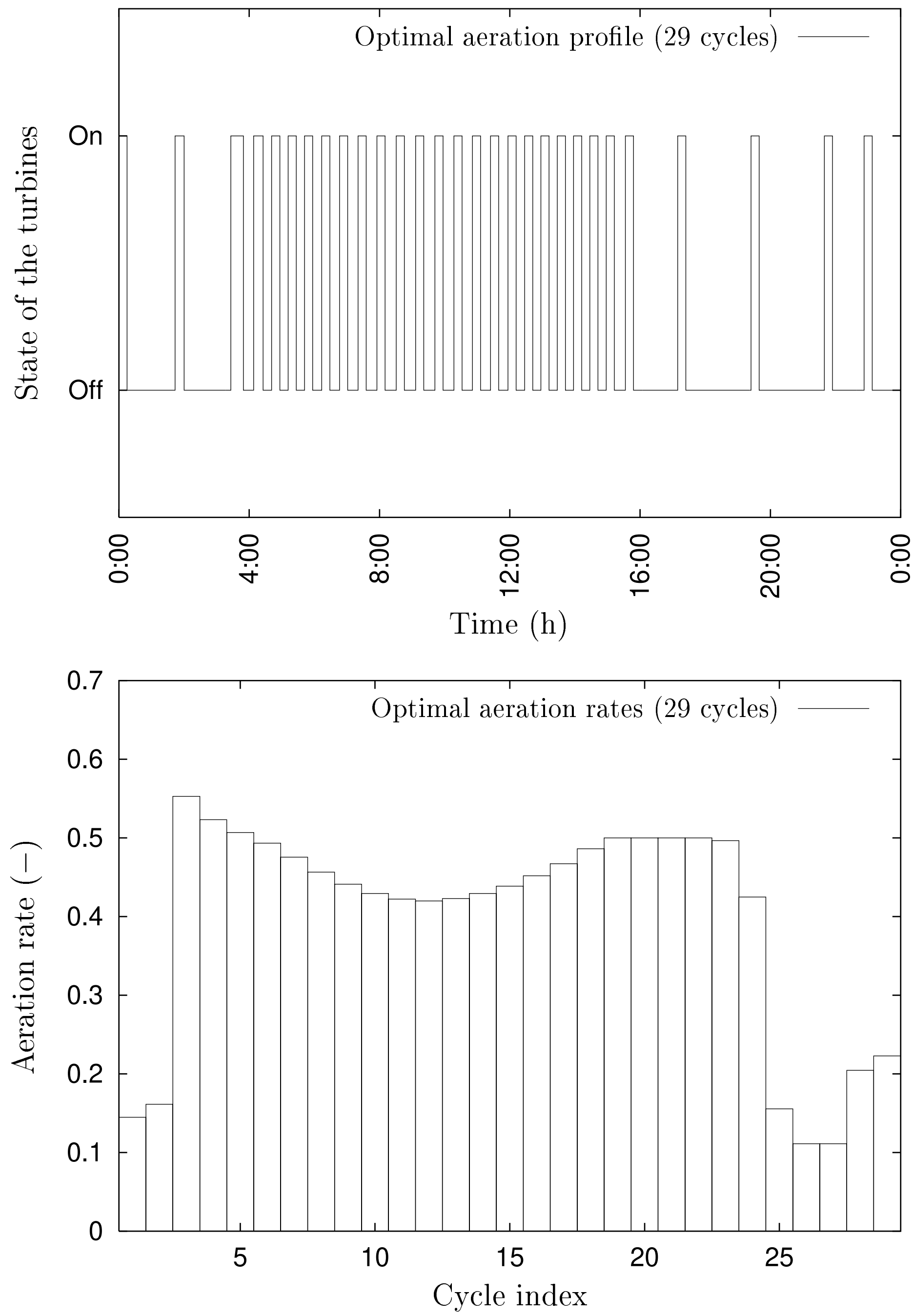

Figure 5: Results of the optimization for 29 cycles a day: optimal aeration policy (upper plot) and optimal aeration rates (lower plot).

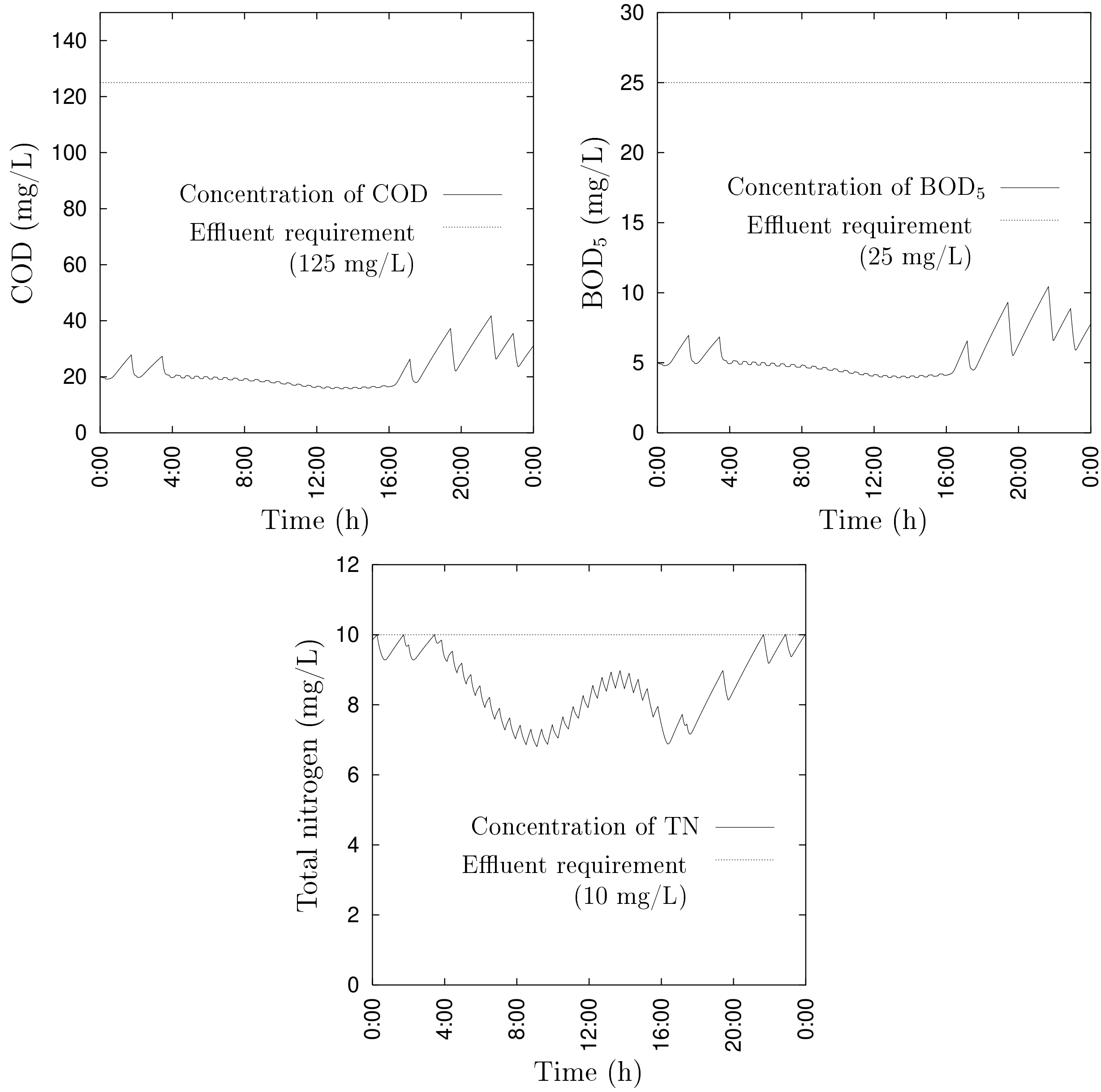

Figure 6: Results of the optimization for 29 cycles a day: COD (upper left plot), BOD_5 (upper right plot) and total nitrogen (lower plot) concentrations *vs.* time.

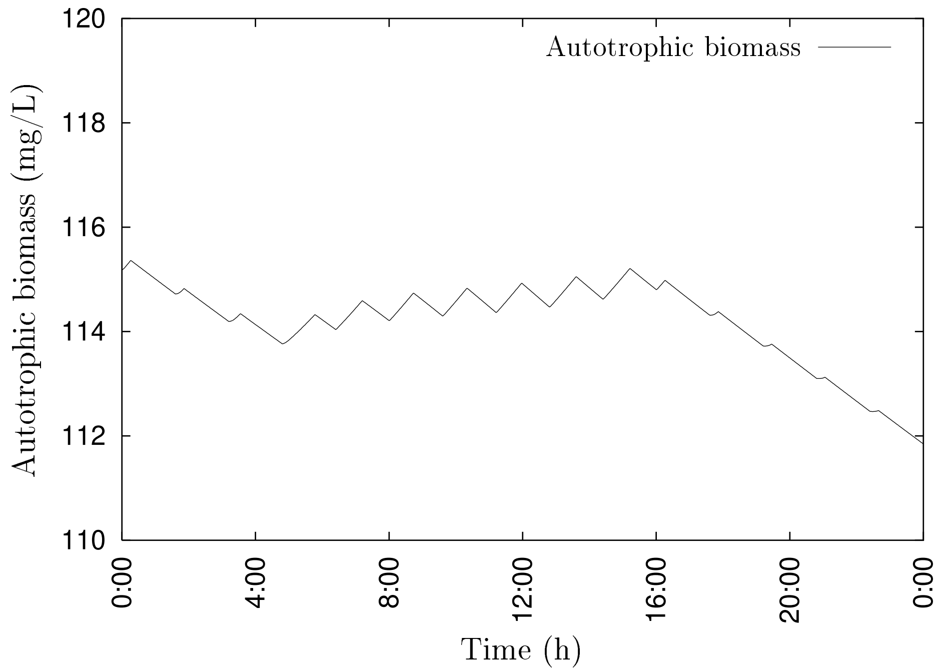

Figure 7: Results of the optimization for 29 cycles a day: autotrophic biomass concentration *vs.* time

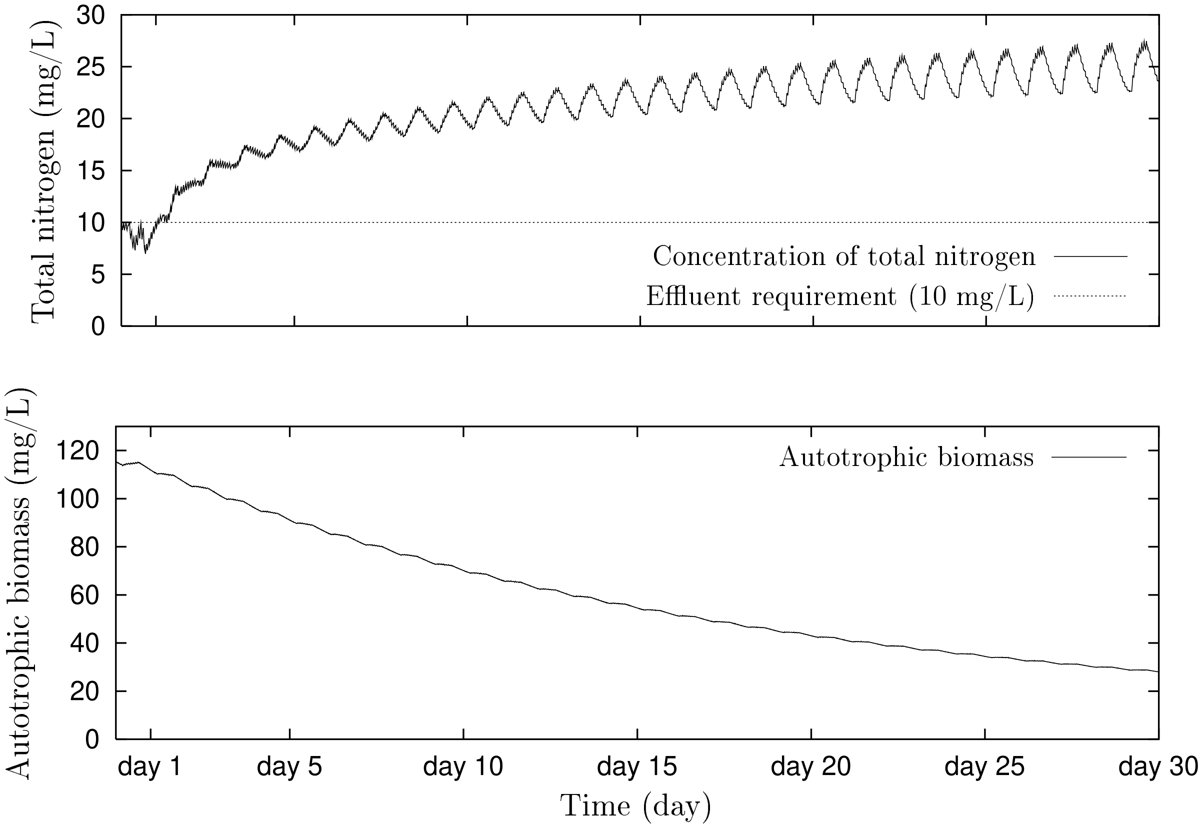

Figure 8: Application of the optimal aeration policy (computed for a 24-hour period) over 30 days: total nitrogen concentration *vs.* time (upper plot) and autotrophic biomass concentration *vs.* time (lower plot).

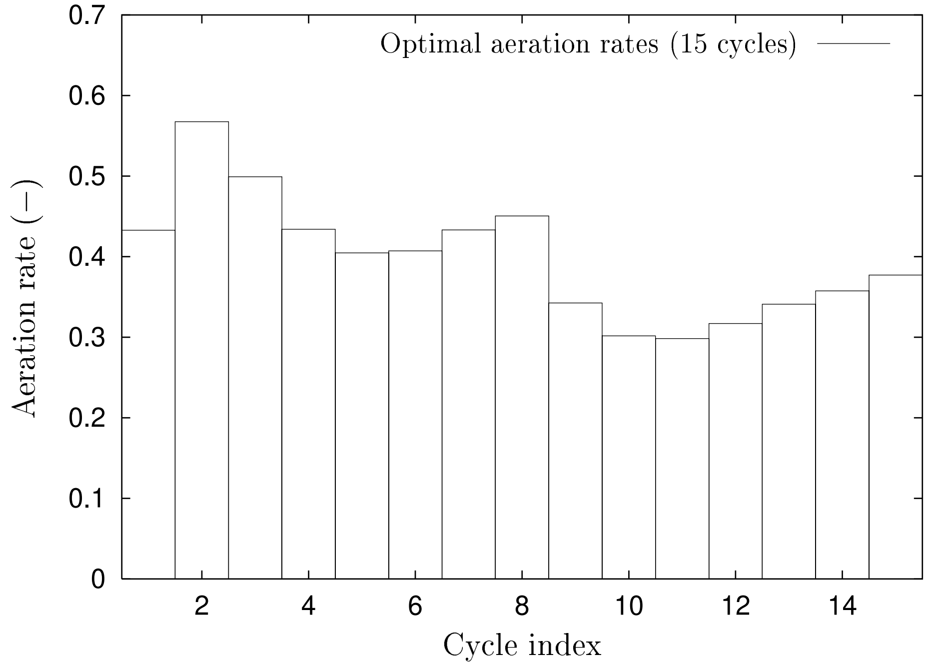

Figure 9: Optimal aeration profile for a 15-cycle optimisation over 60 days.

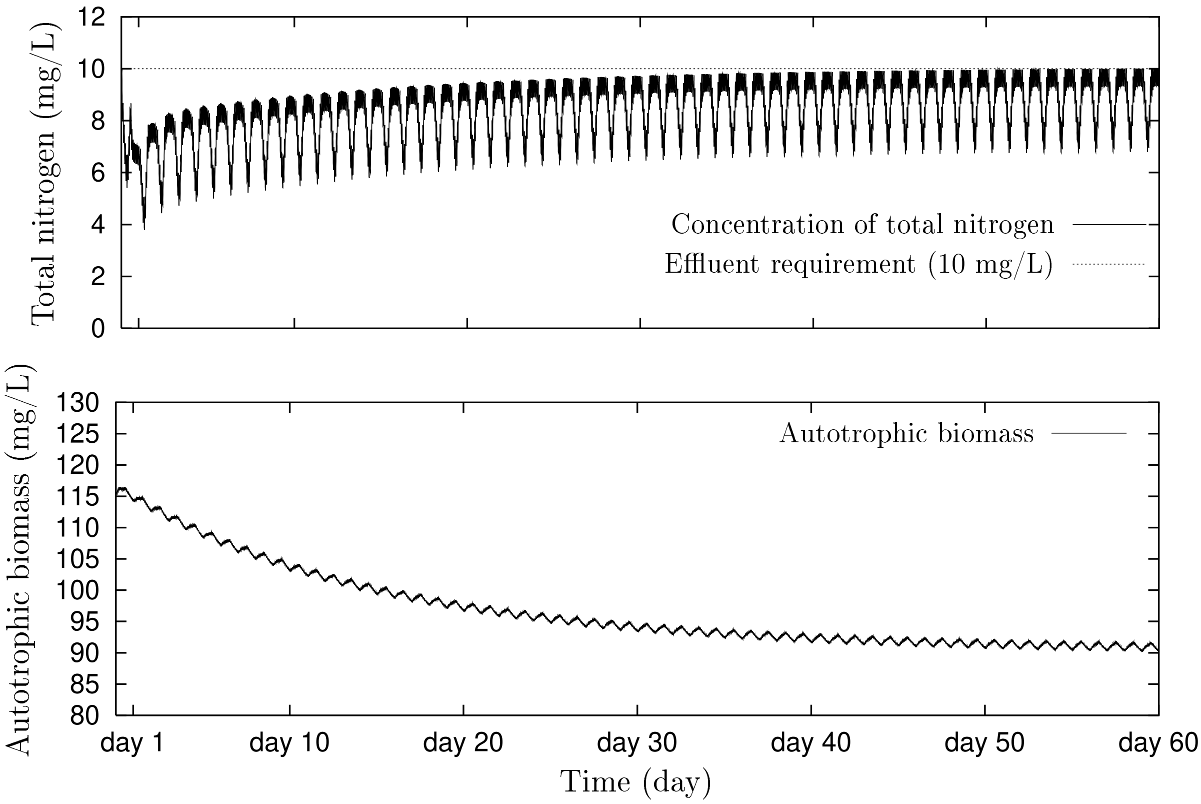

Figure 10: Results of the long-term optimization over 60 days : total nitrogen concentration *vs.* time (upper plot) and autotrophic biomass concentration *vs.* time (lower plot).

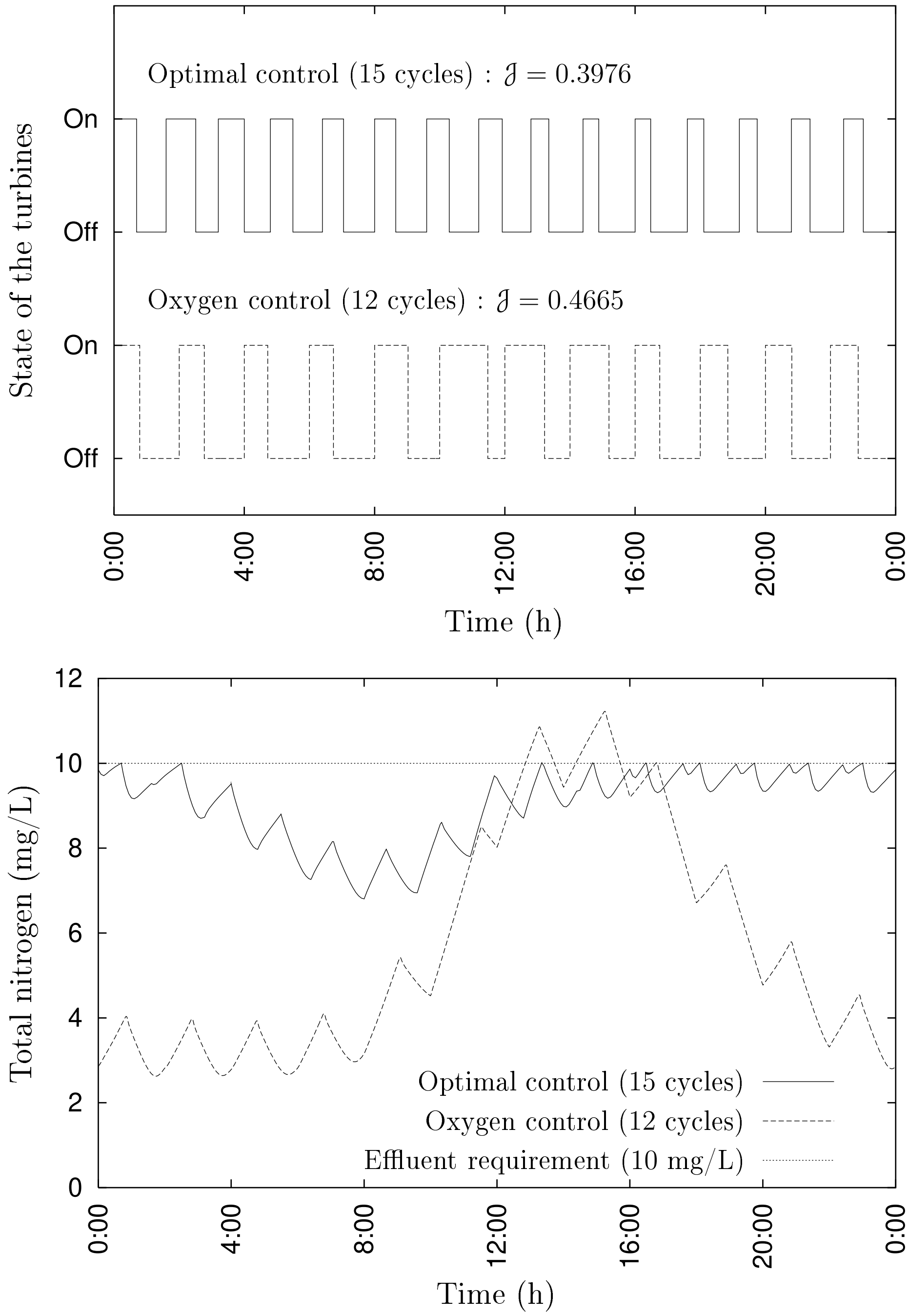

Figure 11: Comparison between optimal and rule-based control strategies : aeration (upper plot) and total nitrogen concentration (lower plot) profiles.